UIDE

Powered by
Arizona State University

# ING. MECATRÓNICA

## SUBMITTED IN PARTIAL FULFILLMENT OF THE REQUIREMENTS FOR THE DEGREE OF MECHATRONIC ENGINEER

**AUTHOR:** Erick Ramiro Peñaherrera Vega

**TUTOR:** Ing. Gabriela Andaluz, MSc.

# DESIGN AND IMPLEMENTATION OF A DISINFECTION SYSTEM FOR DENTAL CHAIRS AIDED BY VISION WITH ARTIFICIAL INTELLIGENCE

QUITO – ECUADOR | 2023

# CERTIFICATE OF AUTHORSHIP

I, Erick Ramiro Peñaherrera Vega, hereby declare that this submission is my own work, it has not been previously submitted for any degree or professional qualification and that the detailed bibliography has been consulted.

I transfer my intellectual property rights to the Universidad Internacional del Ecuador, to be published and divulged on the internet, according to the provisions of the Ley de Propiedad Intelectual, its regulations and other legal dispositions.

**Erick Ramiro Peñaherrera Vega**

# ACKNOWLEDGMENTS

This work would not have been possible without the constant support of my parents, Ximena and Ramiro whose love and guidance have helped me achieve this goal and to whom I would like to dedicate this project. I can not express how deeply grateful I am to them, for they have always sought to give the best for me, and whose sacrifice has allowed me to have this opportunity. Without them I would not have been able to complete this project, nor would I have made it through my degree. I would like to thank my grandparents, especially my grandfather Roberto, who was always there to correct, support, guide, love and take care of me ever since I was little, and who ultimately was my greatest role model. I wish to thank my loving and supportive girlfriend, Doménica, who provided unending love and inspiration throughout this journey. I am also grateful to my friends and classmates who made these years a fun experience, and whose support and friendship was invaluable as well.

# CONTENTS

# LIST OF FIGURES

# LIST OF TABLES

# DESIGN AND MATERIALS SELECTION

## 1. Project's Technical Requirements

The project will have the following scope:

- The proposed system will be able to recognize, using ultraviolet light, if the dental chair area is disinfected, and if not, it will proceed to spray the area with a disinfectant solution.
- The disinfection system will have a mechanical structure type arm, which will be fixedly coupled to the chair and will allow it to move and cover the entire chair area to detect and disinfect.
- The system will have a camera that will allow, through an artificial vision algorithm, to identify stains on the chair when illuminated by UV light.
- The system will have a panel that will allow the user to start the process, pause or stop it at any time.
- A control unit will be used to automate the entire system, which will allow reading the inputs and outputs of the variables involved in the process.

In Table 1 the requirements for design are described.

**Table 1.** Project's Requirements

| **Parameter** | **Description** |
|---|---|
| Portability | The project must be portable, meaning it can be transported to and from the dental office |
| Adaptability | It must be adaptable to the dental chair Fedesa Astral Lux |
| Actuation | DC motors |
| Image Input Device | USB Web Cam |

# 2. Alternatives Analysis

## 2.1. Mechanism / Structure

The main structure of the project is a robotic manipulator because it allows speeding up activities, tasks and functions that require repeatability and precision. The different possible configurations for the project are analyzed below.

### 2.1.1. Articulated Robot

The articulated robot has at least three joints that rotate on themselves, allowing it to carry out more complex tasks. Articulated robots are extremely versatile, making them perhaps the most common type of industrial robot. Companies often choose articulated robots for their automation needs because they offer many key benefits for optimizing processes [1].

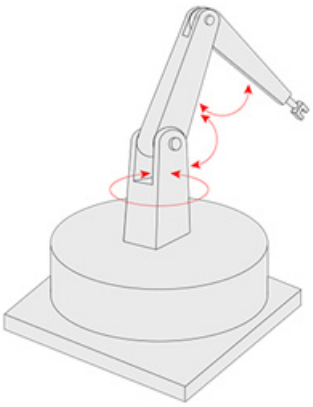

**Figure 1.** Articulated Robot [1]

### 2.1.2. SCARA

A SCARA robot can rotate in two joints and has a linear joint. It is ”supported” in the horizontal plane and rigid in the vertical. This is why its name contains the phrase ”selective compliance.” The SCARA robotic arm design is very similar to a human arm. The first axis (X axis) moves horizontally. The second (Y axis), mounted on the first axis, allows us to position in two dimensions. The third (Z axis) is made up of a spindle that adds the vertical component. The fourth axis is the rotation of the spindle itself, which allows the product to be oriented in the desired position on the plane [2].

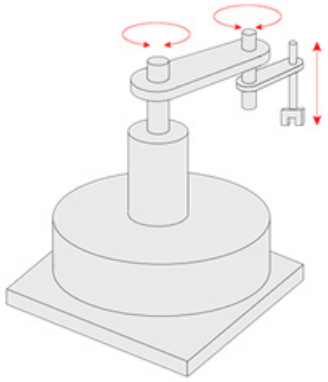

**Figure 2.** SCARA Robot [2]

### 2.1.3. Polar Robot

Polar/Spherical robots are robot configurations with a combined linear joint and two rotary joints, with an arm connected to a robotic base and a rotary joint. Also known as spherical robots, the axes create a spherical workspace and a polar coordinate system [3].

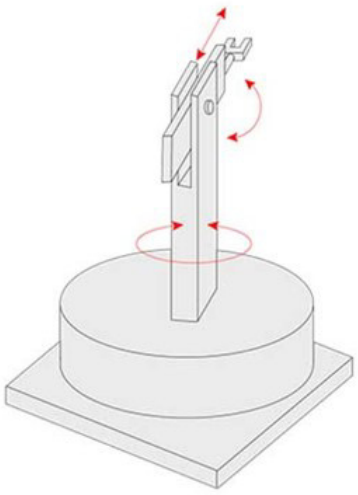

**Figure 3.** Polar Robot [3]

Each of the options above present advantages and disadvantages for this application, which are analyzed following the criteria, which have weights asigned to each one:

- Controlability - 25%
- Degrees of freedom - 20%

- Workspace - 25%
- Flexibility - 30%

Each option is qualified with a value from 1 to 5, the results are presented in Table 2 below.

**Table 2.** Mechanism Alternatives Comparison

| | Controlability | | DoF | | Workspace | | Flexibility | | Total |
|---|---|---|---|---|---|---|---|---|---|
| Weight | 0.25 | | 0.2 | | 0.25 | | 0.3 | | 1 |
| Opción 1 | 3 | 0.75 | 3 | 0.6 | 4 | 1 | 4 | 1.2 | 3.55 |
| Opción 2 | 4 | 1 | 2 | 0.4 | 3 | 0.75 | 3 | 0.9 | 3.05 |
| Opción 3 | 3 | 0.75 | 2 | 0.4 | 3 | 0.75 | 3 | 0.9 | 2.8 |

By observing each type of arm, it can be concluded that the most appropriate structure for this application is an Articulated Robot, due to the advantages it has over the other options, such as versatility, controllability, that the work space can be obtained sufficiently wide with fewer degrees of freedom, which means fewer motors, better control, and lower price.

## 2.2. Actuators Selection

### 2.2.1. Motor Selection

The purpose of the motors in the project is to move the links of the arm, thus each joint must have a motor.

**Option 1:** NEMA 17

A NEMA 17 stepper motor is a kind of motor that can be programmed to rotate in exact steps or increments, various devices like CNC machines and robots usually include stepper motors thanks to its small size and good torque [4]. Its specifications are described in Table 12.

**Option 2:** FT5325M Servo motor

A servo motor is a type of electric motor that is commonly used in motion control applications. Because they use feedback to monitor and adjust their position, they can

**Table 3.** NEMA 17 Stepper Motor's Specifications [4]

| Parameter | Value |
|---|---|
| Mass | 225$\mathrm{g}$ |
| Dimensions | 40.7 x 19.7 x 42.9 $\mathrm{mm}$ |
| Voltage | 12$\mathrm{V}$ |
| Rated current | 2.4$\mathrm{A}$ |
| Holding torque | 4.8 $\mathrm{kgf \cdot cm}$ |
| Rated torque | 4.8$\mathrm{kgf \cdot cm}$ |
| Price | $15 |

maintain a precise position even in the presence of external forces or load changes. They are also relatively fast and responsive, with the ability to change position quickly [5]. The FT5325M servo's specifications are described in Table 4 below.

**Table 4.** FT5325M Servo motor's Specifications [5]

| Parameter | Value |
|---|---|
| Mass | 67$\mathrm{g}$ |
| Dimensions | 40 x 20.5 x 40.5 $\mathrm{mm}$ |
| Voltage | 4.8 $\mathrm{V}$ - 7.2 $\mathrm{V}$ |
| Rated current | 210 $\mathrm{mA}$ – 260 $\mathrm{mA}$ |
| Rated torque | 20.5 $\mathrm{kgf \cdot cm}$ (4.8 $\mathrm{V}$ )/ 22.8 $\mathrm{kgf \cdot cm}$ (7.2 $\mathrm{V}$) |
| Price | $29 |

Each of the options above present advantages and disadvantages for this application, which are analyzed following the criteria, which have weights asigned to each one:

- Controlability - 25%
- Performance - 20%
- Weight - 25%
- Price - 30%

Each option is qualified with a value from 1 to 5, the results are presented in Table 5 below.

For the selection of the motor, the force necessary to move each link of the arm must be taken into account. Approximate values of the weight of the links, elbows and

**Table 5.** Motor Alternatives Comparison

| | Controlability | | Performance | | Weight | | Price | | Total |
|---|---|---|---|---|---|---|---|---|---|
| Weight | 0.25 | | 0.2 | | 0.25 | | 0.3 | | 1 |
| Opción 1 | 2 | 0.4 | 2 | 0.6 | 2 | 0.4 | 4 | 1.2 | 2.6 |
| Opción 2 | 3 | 0.6 | 5 | 1.5 | 4 | 0.8 | 3 | 0.9 | 3.8 |

end effector of the arm were taken. For this analysis, approximate weights of the components and arms were considered. Variables $A_1$ and $A_2$ represent the mass of the actuators, $A_3$ the end effector, and $M_1$ and $M_2$ the mass of the arm links and $L_1$ and $L_2$ their length. The torque calculation was carried out to have a better idea of the necessary force that the motors must have to move the arm.

Considering the weight of the motors $67\mathrm{g}$, which the average weight of a DC motor, the weight of the links $70\mathrm{g}$ and the approximate weight of each joint as $140\mathrm{g}$.

$$A_1 = A_2 = 0.067\mathrm{kg} + 0.14\mathrm{kg}$$

$$A_3 = 0.14\mathrm{kg}$$

$$L_1 = L_2 = 0.3\mathrm{m}$$

$$M_1 = M_2 = 0.07\mathrm{kg}$$

Where: $A_1$ and $A_2$: are the masses of the actuators, in $\mathrm{kg}$.

$A_3$: is the mass of the end effector. in $\mathrm{kg}$.

$L_1$ and $L_2$: are the legnths of the links, in $\mathrm{m}$.

$M_1$ and $M_2$: are the masses of the links, in $\mathrm{kg}$.

For the first joint

$$\sum Fx = 0 \tag{1}$$

$$M_1 \cdot g \cdot L_1 + A_2 \cdot g \cdot L_1 + M_2 \cdot g \cdot (L_1 + L_2) + A_3 \cdot g \cdot (L_1 + L_2) - T_1 = 0 \tag{2}$$

Replacing in 2:

$$0.07 \cdot .81 \cdot .3 + 0.2 \cdot 9.81 \cdot .3 + 0.07 \cdot 9.81 \cdot (0.3 + 0.3) + 0.14 \cdot 9.81 \cdot (0.3 + 0.3) = T_1$$

$$T_1 = 2.031\mathrm{Nm}$$

Where:

$T_1$: is the torque generated in the first joint, in $\mathrm{Nm}$

For the second joint

$$\sum Fx = 0 \tag{3}$$

$$M_2 \cdot g \cdot L_2 + A_3 \cdot g \cdot L_2 - T_2 = 0 \tag{4}$$

Replacing:

$$0.07 \cdot 9.81 \cdot 0.3 + 0.14 \cdot 9.81 \cdot 0.3 = T_2$$

$$T_2 = 0.618\mathrm{Nm}$$

Where:

$T_1$: is the torque generated in the first joint, in $\mathrm{Nm}$

Taking these results into account, it can be seen that the selected motor offers enough force.

Motor: FT5325M Servo Motor

Torque: $25\mathrm{kg.cm} = 2.45\mathrm{Nm}$

Regarding the selection of the motor, it can be clearly seen that the best way to drive the robot arm is with servo motors, although they do not have the precision of stepper motors, they make up for it with their ease of use and strength.

### 2.2.2. Pump Selection

A pump is needed to move the disinfecting agent from the reservoir to the nozzle in the end effector, since the reservior is localted in the floor, approximately $1.5\mathrm{m}$ from the end effector, a pump strong enough to suck out the liquid is needed.

**Option 1:** AD20P-1230A Brushless Water Pump

**Table 6.** AD20P-1230A Brushless Water Pump's Specifications [6]

| Parameter | Value |
|---|---|
| Dimensions | $55 \times 35 \times 45\mathrm{mm}$ |
| Voltage | $12\mathrm{V}$ |
| Rated current | $0.35\mathrm{A}$ |
| Flow | $4\mathrm{l/min}$ |
| Max. head | $1\mathrm{m}$ |
| Price | $12 |

**Option 2:** R385 Diaphragm Pump

**Table 7.** R385 Diaphragm Pump's Specifications [7]

| Parameter | Value |
|---|---|
| Dimensions | 90 x 40 x 35mm |
| Voltage | 6 - 12V |
| Rated current | 0.5 - 0.7A |
| Flow | 3 l/min |
| Max. head | 3m |
| Price | $9 |

**Option 3:** LBD WP02 Water Pump

**Table 8.** LBD WP02 Water Pump's Specifications [8]

| Parameter | Value |
|---|---|
| Dimensions | 24 x 33 x 24mm |
| Voltage | 5-9V |
| Rated current | 0.2A |
| Flow | 1.3 - 2 l/min |
| Max. head | 1.1m |
| Price | $4 |

Each of the options above present advantages and disadvantages for this application, which are analyzed following the criteria, which have weights asigned to each one:

- Controlability - 20%
- Performance - 30%
- Size - 20%
- Price - 30%

Each option is qualified with a value from 1 to 5, the results are presented in Table 9 below.

**Table 9.** Pump Alternatives Comparison

| | Controlability | | Performance | | Size | | Price | | Total |
|---|---|---|---|---|---|---|---|---|---|
| Weight | 0.2 | | 0.3 | | 0.2 | | 0.3 | | 1 |
| Opción 1 | 5 | 1 | 3 | 0.9 | 3 | 0.6 | 4 | 1.2 | 3.7 |
| Opción 2 | 5 | 1 | 4 | 1.2 | 4 | 0.8 | 3 | 0.9 | 3.9 |
| Opción 3 | 5 | 1 | 2 | 0.6 | 3 | 0.6 | 5 | 1 | 3.2 |

Because the disinfectant solution reserve will be located on the floor, a pump strong enough to suck the liquid from an approximate height of 1.5m is needed, which any of the first 2 options does, however, the R385 Diaphragm Pump (option 2) is the most compact, which is also an important requirement as space on the arm is limited.

### 2.3. Materials Selection

The parts designed for the mechanical structure of the robot, specifically the joints and base, were manufactured in PLA by 3D printing, since it is not only an easy, fast and relatively cheap way to obtain the parts, but also allows to freely design the 3D model PLA also has relatively high mechanical strength, with excellent optical properties, good processing ability with low shrinkage not causing product deformation. [9] A decision was made to use PVC tubes to act as links, since they are easy to find, affordable and lightweight; yet resistant enough for this project. Both PLA and PVC are suitable for this application given that are easy to work with, cheap, and light but stiff. The mechanical properties of both materials can be seen in Tables 10 and 11 [10].

**Table 10.** PLA's Mechanical Properties [9]

| Properties | Value |
|---|---|
| Young's Modulus [MPa] | 3600 |
| Tensile Strength [MPa] | 70 |
| Flexural Strength [N/mm$^2$] | 98 |
| Density [g/cm$^3$] | 1.25 |
| Melting Temperature [℃] | 145 - 160 |

**Table 11.** PVC's Mechanical Properties [10]

| Properties | Value |
|---|---|
| Young's Modulus [MPa] | 2400 - 6900 |
| Tensile Strength [MPa] | 50 |
| Flexural Strength [N/mm$^2$] | 28 - 97 |
| Density [g/cm$^3$] | 1.27 - 1.55 |

## 3. Mechatronic Design

### 3.1. Mechanic Design

#### 3.1.1. Cantilever Beam Link Analysis

To ensure that the links and joints of the arm would withstand the forces applied to them, an analysis was made considering them as a cantilever beam, as seen on Fig. 4.

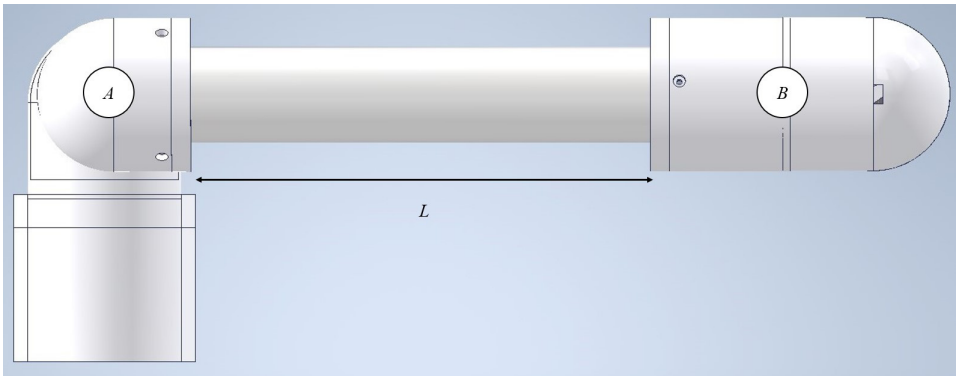


**Figure 4.** Cantilever beam with single load at end

A free body diagram is made in this case, a point charge is analyzed at one end of the link $\mathrm{A}-\mathrm{B}$, as seen on Fig. 5.

Where:

$A$: is the fixed end of the beam.

$B$: is the end where the force is applied.


**Figure 5.** Free body diagram of the cantilever beam with single load at end

In order to obtain the total load at the end of the link a mass of $0.14\mathrm{kg}$ is considered, and applying (5) we get:

$$F = m \cdot g \tag{5}$$

Where:

$F$: is the total load, in $\mathrm{N}$.

$m$: is the mass of the end effector, in $\mathrm{kg}$.

$g$: is the gravity, in $\mathrm{m/s^2}$.

$$F = 0.14\mathrm{kg} \cdot 9.81\mathrm{m/s^2}$$

$$F = 1.37\mathrm{N}$$

This result can be multiplied by a safety factor of 1.5, which is the value for applications were the environment is constant and the loads are easily obtained. [11]

Thus the total load in the link would be:

$$F_s = F \cdot \mu \tag{6}$$

Where:

$F_s$: is the corrected load applied at the end of the link, in $\mathrm{N}$.

$\mu$: is the safety factor, dimensionless.

$$F_s = 1.37\text{N} \cdot 1.5$$

$$F_s = 2.06\text{N}$$

The maximum moment at the fixed can be obtained with [12]:

$$M_{max} = F_s \cdot L \tag{7}$$

$$F_s = 2.06\text{N}$$

$$L = 300\text{mm}$$

Replacing in (7):

$$M_{max} = 2.06\text{N} \cdot 300\text{mm}$$

$$M_{max} = 618\text{Nmm}$$

The maximum deflection at the end of the cantilever beam can be expressed as [12]:

$$\sigma_B = \frac{F \cdot L^3}{3 \cdot E \cdot I} \tag{8}$$

Where:

$\sigma_B$: is the maximum deflection, in $\text{mm}$.

$E$: is the Young's Modulus, in $\text{GPa}$. Obtained from Table 11.

$I$: is the area moment of inertia, in $\text{mm}^4$.

$$E = 6.9\text{GPa}$$

$$I = \frac{\pi(d_o^4 - d_i^4)}{64} \tag{9}$$

Where:

$d_i$: is the inner diameter, in $\mathrm{mm}$.

$d_i$: is the inner diameter, in $\mathrm{mm}$.

Using (9) the second moment of inertia can be obtained [12].

$$I = \frac{\pi(50\mathrm{mm}^4 - 49\mathrm{mm}^4)}{64}$$

$$I = 23817.2\mathrm{mm}^4$$

Replacing in (8):

$$\sigma_B = \frac{1.37\mathrm{N} \cdot (300\mathrm{mm})^3}{3 \cdot 6900\mathrm{N/mm^2} \cdot 23817.2\mathrm{mm}^4}$$

$$\sigma_B = 0.075\mathrm{mm}$$

The stress in a bending beam can be expressed as [12]:

$$\sigma = \frac{y \cdot M}{I} \tag{10}$$

Where:

$y$: is the distance to point from neutral axis, in $\mathrm{mm}$..

$M$: is the bending moment, in $\mathrm{Nmm}$.

$I$: is the area moment of inertia, in $\mathrm{mm}^4$..

$$\sigma = \frac{25\mathrm{mm} \cdot 411\mathrm{Nmm}}{23817.2\mathrm{mm}^4}$$

$$\sigma = 0.43\mathrm{MPa}$$

The maximum stress in the bending beam is $0.43\mathrm{MPa}$ which is lower than the ultimate tensile strength for PVC ($50\mathrm{MPa}$).

In Figure 6 the diagrams of shear forces and bending moments are presented.

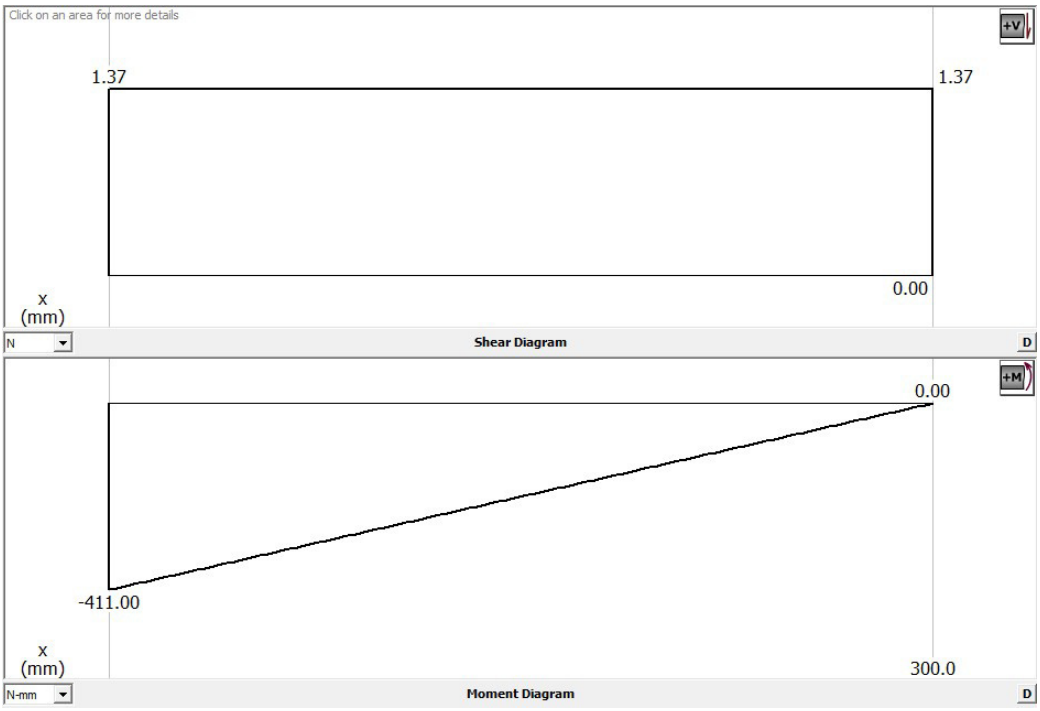


**Figure 6.** Diagrams of Shear Forces and Bending Moments for the Links

### 3.1.2. Finite Element Analysis

Once both the stress and maximum deflection were calculated a finite elements analysis (FEA) was carried out in Autodesk Inventor in order to corroborate this results applying the load of $2.06\mathrm{N}$ , in Figures 7 and 8 can be seen that the results are quite close, which confirms the calculations made.

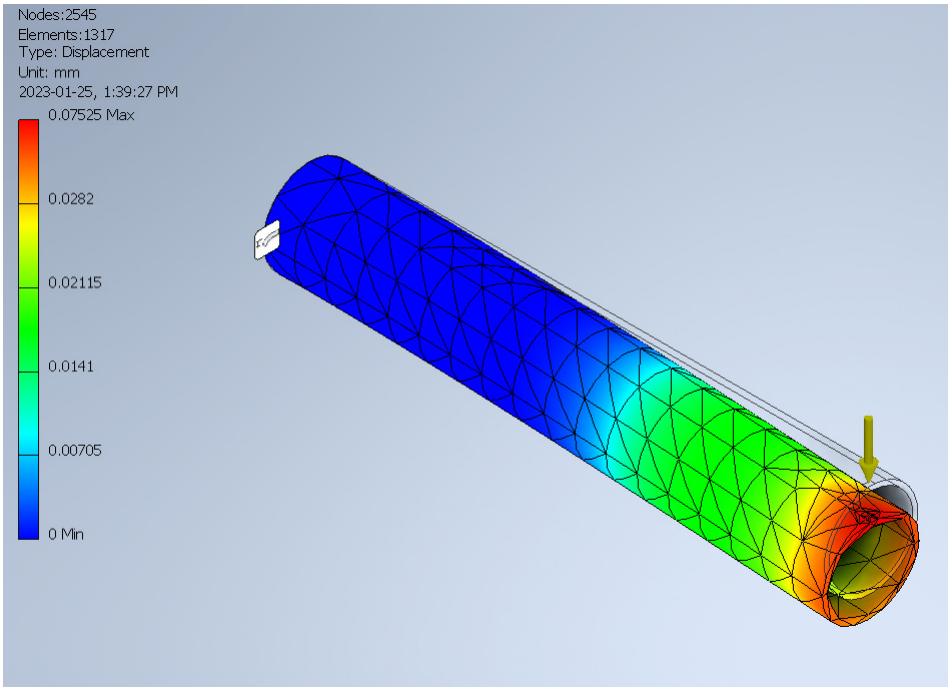


**Figure 7.** Displacement obtained in the Finite Element Analysis

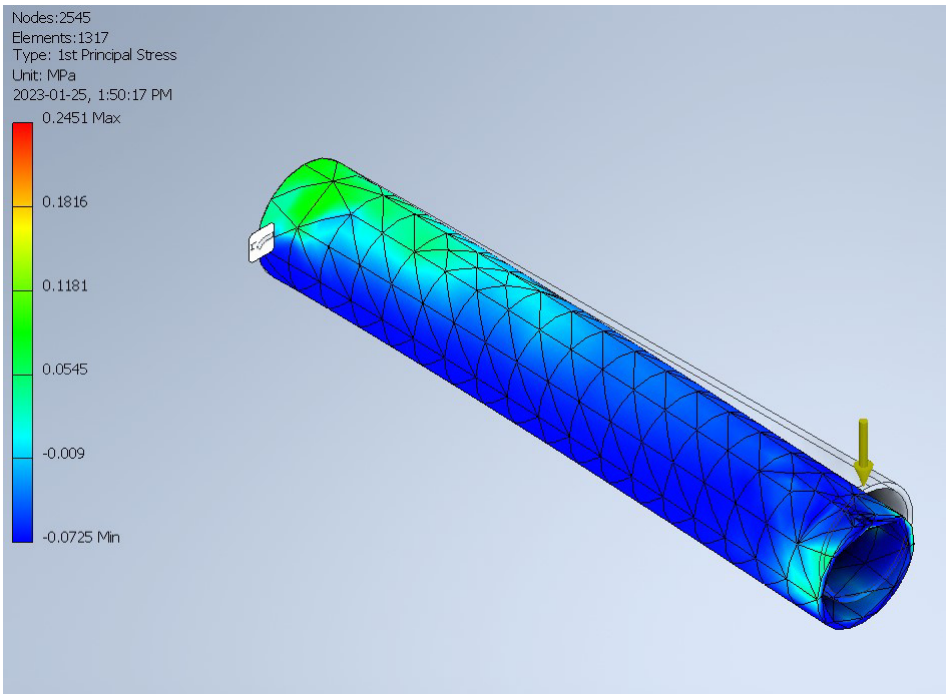


**Figure 8.** Maximum Stress obtained in the Finite Element Analysis

### 3.1.3. Final Design

In Figure 9 the final 3D model in Autodesk Inventor is shown.

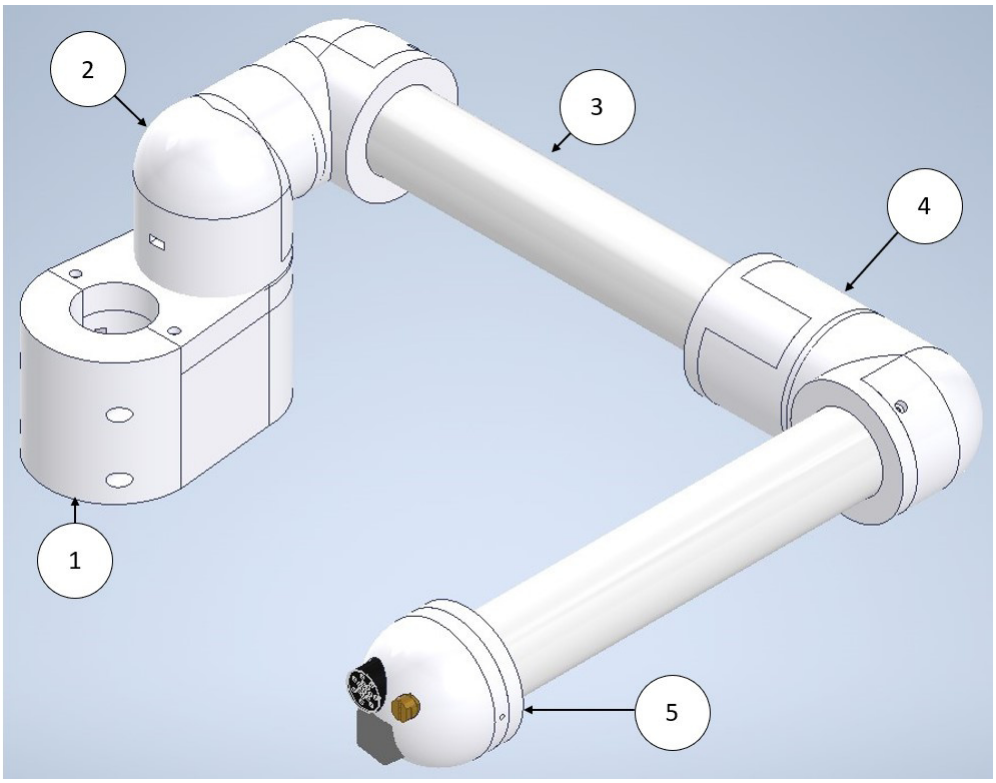


**Figure 9.** Final CAD Model

**Table 12.** Parts of the Disinfecting System

| Number | Description |
|---|---|
| 1 | Support / Base |
| 2 | First joint |
| 3 | Link |
| 4 | Second joint |
| 5 | End effector |

## 3.2. Electronic Design

The electronic design covers the sizing and selection of the necessary components that comprise the project. The projec'ts architecture is better understood in the diagram of Fig. 10.

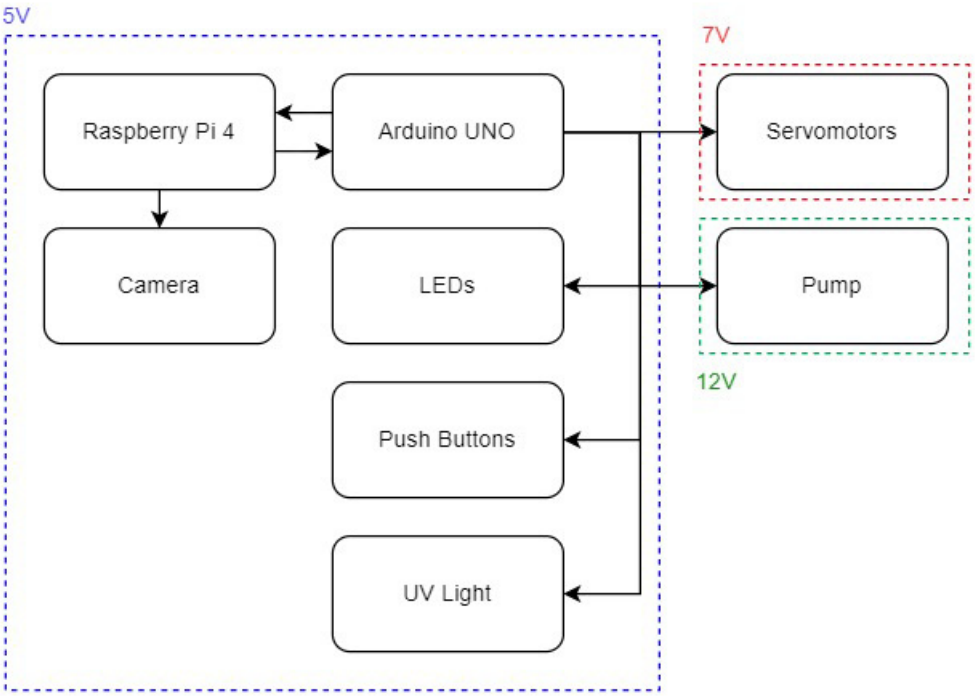


**Figure 10.** Electric components architecture

### 3.2.1. Micro-controller Selection

For the automation of the entire system, a control unit will be used to read the inputs and outputs of the variables involved in the process. In order to select an adequate micro-controller the following requirements were taken into account.

- 3 digital input pins.

- 5 digital output pins.
- 3 pins for PWM signals.
- 1 USB port.
- OpenCV / Python compatibility.
- Serial communication capabilities.

Given this requirements the possible options are:

**Option 1:** Raspberry Pi 4

The Raspberry Pi 4 is a minicomputer with a 64-bit quad-core processor and 1Gb of memory, which makes it good for image processing applications. It has USB compatibility that allows to connect devices such as cameras, as well as stablishin serial communication with other controllers [13].

**Option 2:** Arduino UNO

Arduino UNO is a microcontroller that uses the ATmega328P. It has 14 digital I/O pins, 6 of which can be used as PWM outputs, 6 analog inputs, and a USB connection [14].

A decision was made to use both of these micro-controllers, since both offer benefits to the project. The Raspberry Pi 4, seen in Fig. 11, is used to handle all the more processor-heavy work from the artificial vision, and the Arduino UNO, seen in Fig. 12, is used to code and implement the control for the actuators. These micro-controller are connected via the USB port and use serial communication to work along each other.

### 3.2.2. Camera Selection

In order to select an appropiate camera for this project, the following requierements must be met:

- Small dimensions.
- At least 720p resolution.

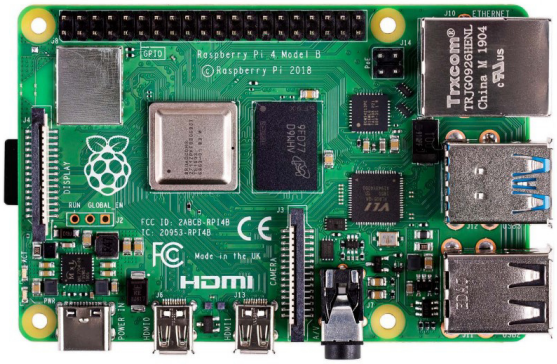


**Figure 11.** Raspberry Pi 4 [13]

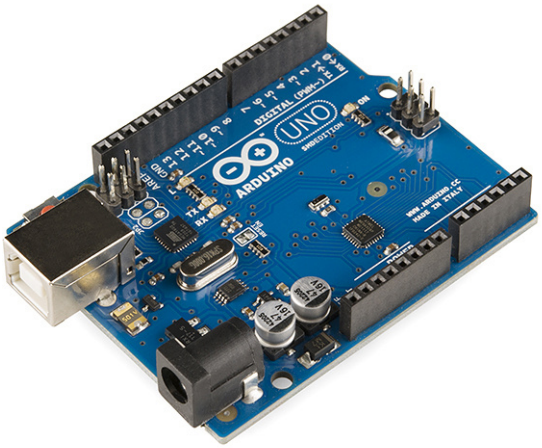


**Figure 12.** Arduino UNO [14]

- USB powered.

Taking there requirements into consideration, the available options are:

**Option 1:** SQ11 Mini Camera, seen in Fig. 13.

Parameters:

- Video resolution: 1920 X 1080p / 1280 X 720p
- Frame rate: 15 / 30 FPS
- Viewing angle: 140°
- Dimensions: 24 X 24 X 24 mm
- Power: 5V USB powered

- Price: $9

**Figure 13.** SQ11 Mini Camera

**Option 2:** A9 Camera, seen in Fig. 14.

Parameters:

- Video resolution: 1920 X 1080p / 1280 X 720p
- Frame rate: 24 FPS
- Viewing angle: 150°
- Dimensions: 45 X 45 X 25 mm
- Power: 5V USB powered
- Price: $15


**Figure 14.** A9 Mini HD Camera

While both options met the established requirements, the SQ11 was chosen due to its smaller size and lower cost.

### 3.2.3. UV Light Selection

For the UV light the only requirements were for it to be small sized, so not many options were considered. The selected light was a UV LED light torch, with 9 bulbs and $400\text{nm}$ wavelength, powered by 5V.

### 3.2.4. Firing Circuit for the Pump

In order to control the smaller components, such as the pump, that do not need as much current as the other elements a transistor as a switch was used, as seen on Fig. 15 what also allowed to be easily controlled from the micro controller. The selected transistor was the TIP22 since it is rated to handle a current up to 5A, which was enough to handle the current provided by the regulators.

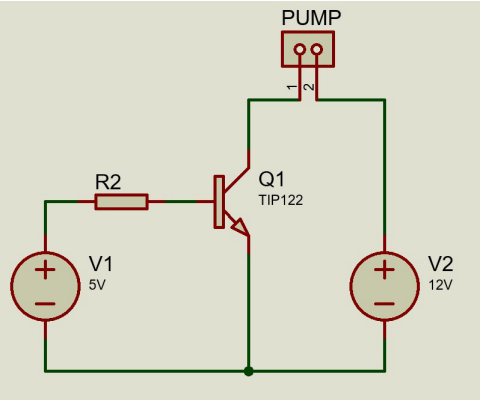


**Figure 15.** Transistor as a switch circuit

From the TIP122 Darlington Transistor's datasheet [15] we know:

$$I_cMax = 800\text{mA}$$

$$\beta = 100$$

Where:

$I_cMax$: is the maximum rating of the base current in the transistor, in $\text{mA}$.

$\beta$: is the transistor's current gain.

The Current of the collector divided by the current in the base of the transistor will be equal to $\beta$, as Eq. 11 shows.

$$\frac{I_c}{I_b} = \beta \tag{11}$$

Where:

$I_c$: is the current in the colector of the transistor, in $\mathrm{mA}$.

$I_b$: is the current in the base of the transistor, in $\mathrm{mA}$.

Since the Pump needs $700\mathrm{mA}$, that will be the current assumed for the collector of the transistor.

$$100 = \frac{0.7}{I_b}$$

$$I_b = \frac{0.7}{100} = 0.007A = 7\mathrm{mA}$$

Applying the sum of voltages equal to zero in M1 we got the value of the voltage in R2 as Eq. 12 shows.

$$5V - VR2 - VBE = 0 \tag{12}$$

$$VR2 = 4.3V$$

Applying Ohm's law we can get the value of the R2 as shown in Eq. 13.

$$R2 = \frac{VR2}{I_b} \tag{13}$$

$$R2 = \frac{4.3V}{0.007} = 614.29\Omega$$

This value is later used to design the ciruit for the PCB.

### 3.2.5. Power Supply Unit Sizing

In order to select an adequate power supply for the project is necessary to know exactly how much voltage and current each of the components require, so to estimate the total consumption of the system as a whole. In Table 13 are detailed the different electronic components and their power requirements.

The total estimated current draw for the project is $7.52\mathrm{A}$, taking this value into account

**Table 13.** Power Consumption of each Electronic Component

| | Component | Quantity | Voltage [V] | Current [A] | Total Current |
|---|---|---|---|---|---|
| 1 | Arduino UNO | 1 | 5 | 0.02 | 0.02 |
| 2 | Raspberry Pi 4 | 1 | 5 | 3 | 3 |
| 3 | FT5325M Servo Motor | 3 | 7 | 1.2 | 3.6 |
| 4 | R385Diaphragm Pump | 1 | 12 | 0.7 | 0.7 |
| 5 | UV Light | 1 | 5 | 0.05 | 0.05 |
| 6 | USB Web Cam | 1 | 5 | 0.15 | 0.15 |
| Total | | | | | 7.52 |

the selected power supply was the S-120-12 which is a $12\mathrm{V} - 10\mathrm{A}$ switching power supply, this provides enough current to power every element even when they are all working at the same time. The voltage however it too much for certain components, due to this voltage regulators were used, specifically the XL4005, which is a DC-DC step-down that can output up to $30\mathrm{V}$ at $6\mathrm{A}$, two of these were used for the motors and the micro controllers, which work at $7\mathrm{V}$ and $5\mathrm{V}$ respectively.

Having done this calculations, the components are summarized in Table 14 below.

**Table 14.** Parts of the Disinfecting System

| **Component** | **Description** | **Quantity** |
|---|---|---|
| Raspberry Pi 4 | Micro-controller | 1 |
| Arduino UNO | Micro-controller | 1 |
| USB Camera | Web camera / image input device | 1 |
| FT5325M Servo Motor | $25\mathrm{kg}\cdot\mathrm{cm}$ servo motors | 3 |
| R385 Diaphragm Pump | $12\mathrm{V}$ water pump | 1 |
| UV Light | $5\mathrm{V}$ UV LED light | 1 |
| Resistors | $600\Omega$ resistors | 2 |
| TIP 122 | NPN Darlignton Transistor | 1 |
| Push buttons | Buttons | 3 |
| 4005XL Voltage regulators | $5\mathrm{V}$ and $7\mathrm{V}$ Step downs | 2 |

Finally, once all the components were sized and selected, a case to house all the electronic elements was designed, as seen on Figures 16 and 17.

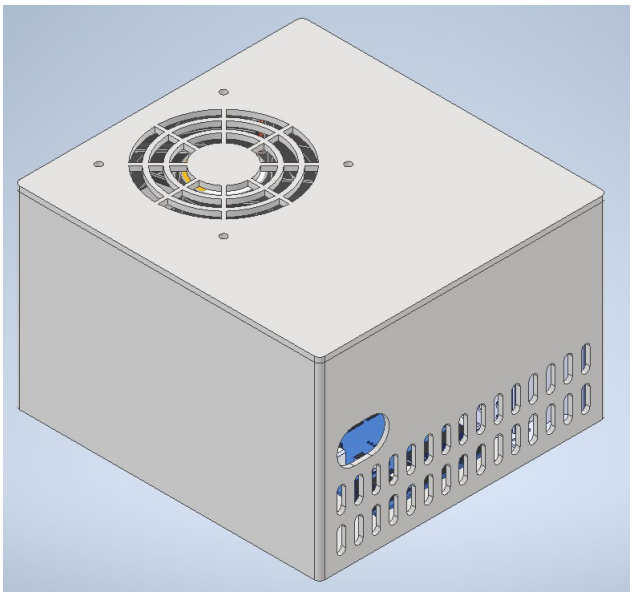

**Figure 16.** Circuit box designed in Inventor

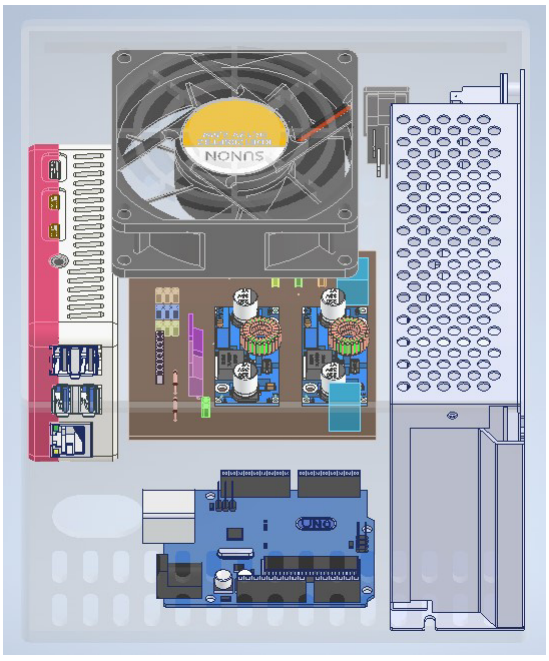

**Figure 17.** Internal view of the circuit box

## 3.3. Robot Arm Programming

### 3.3.1. Kinematic Analysis

Kinematic analysis of robot arms is the study of the motion and behavior of robot arms without taking into account the forces that cause the motion. It involves the use of mathematical models to describe the movement of the robot's joints, links, and end-effectors. This includes determining the position, velocity, and acceleration of the robot's various

parts, as well as the relationships between them [16].

One important aspect of kinematic analysis is the use of Denavit-Hartenberg (DH) notation, which is a method of describing the relative positioning of the joints and links in a robot arm. This notation allows for the creation of a kinematic model of the robot arm, which can be used to determine the forward and inverse kinematics of the arm. Forward kinematics is the process of determining the position and orientation of the end-effector of the robot arm based on the positions of its joints. Inverse kinematics is the opposite, it's the process of determining the joint positions that are required to achieve a certain end-effector position and orientation [16].

Other important areas of study in kinematic analysis of robot arms include trajectory planning, which involves determining the path the robot arm should follow to reach a desired position, and singularity analysis, which is the study of the points in the robot's workspace where its kinematic model becomes singular, or degenerate, which can cause issues with control and stability. Overall, kinematic analysis of robot arms is a fundamental and crucial step in the design, control, and programming of robots. It enables the understanding of the movement, and can help in the design of more efficient and accurate robotic systems [17].

### 3.3.2. Denavit–Hartenberg Parameters

A robot manipulator's joints are each given coordinate frames in a straightforward and consistent manner using the Denavit-Hartenberg method. A homogeneous transformation matrix that is relevant for the manipulator's forward and inverse kinematics may be defined using these parameters. Each of the robot's joints is broken down into four parameters by the DH parameters, each measured in relation to the preceding joint. They are computed using the aforementioned ”common normal.” The common normal has a length of zero if the prior z-axis overlaps the present z-axis, which is frequently the case. [18] In my case the manipulator is a Spherical RRR Manipulator, and in Figures 18 and 19 the axis and angles are defined.

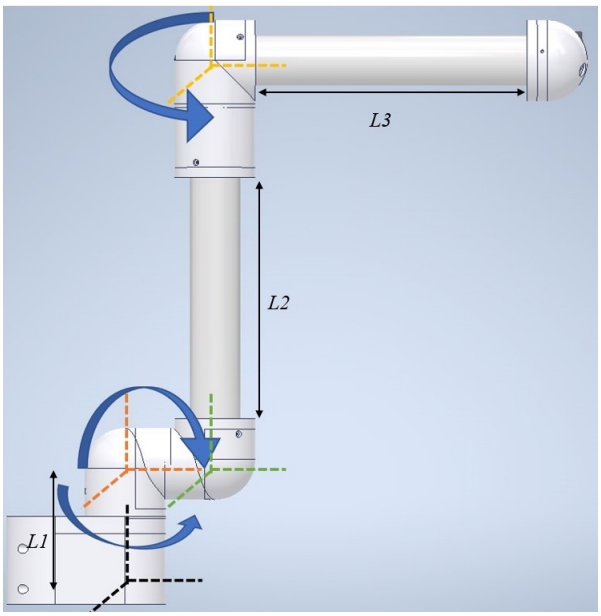


**Figure 18.** Axis and rotations defined in the CAD model

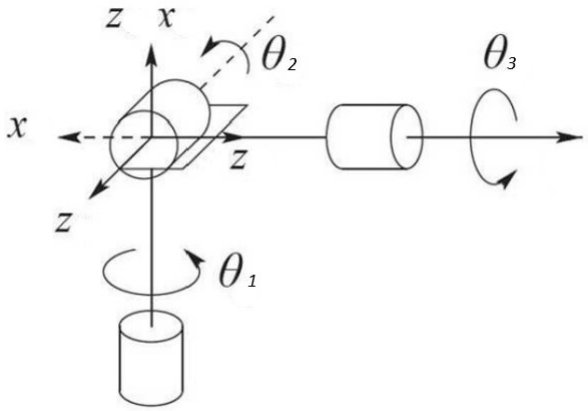


**Figure 19.** Rotation angles defined in a RRR manipulator diagram

Once the axis and angles had been figured out, the DH parameters can be obtained, seen in Table 15.

**Table 15.** Denavit–Hartenberg Parameters

| Link | $a_i$ | $\alpha$ | $d_i$ | $\theta_i$ |
|---|---|---|---|---|
| 1 | 10 | 90 | $d_1$ | $\theta 1$ |
| 2 | 30 | -90 | $d_2$ | $\theta 2$ |
| 3 | 30 | 0 | $d_3$ | $\theta 3$ |

A simulation of the arm was carried out in MATLAB using Peter Corke's Robotics Toolbox, in which the Denavit–Hartenberg Parameters were computed and a model of the robot was obtained, as seen in Figures 20 and 21.

```
robot =

noname (3 axis, RRR, stdDH, fastRNE)

+---+-----------+-----------+-----------+-----------+-----------+
| j |     theta |         d |         a |     alpha |    offset |
+---+-----------+-----------+-----------+-----------+-----------+
|  1|         q1|         10|          0|      1.571|          0|
|  2|         q2|         30|          0|     -1.571|          0|
|  3|         q3|         30|         30|          0|          0|
+---+-----------+-----------+-----------+-----------+-----------+

grav =    0  base = 1  0  0  0   tool =  1  0  0  0
          0          0  1  0  0           0  1  0  0
       9.81          0  0  1  0           0  0  1  0
                     0  0  0  1           0  0  0  1
```

**Figure 20.** Denavit–Hartenberg Parameters in MATLAB

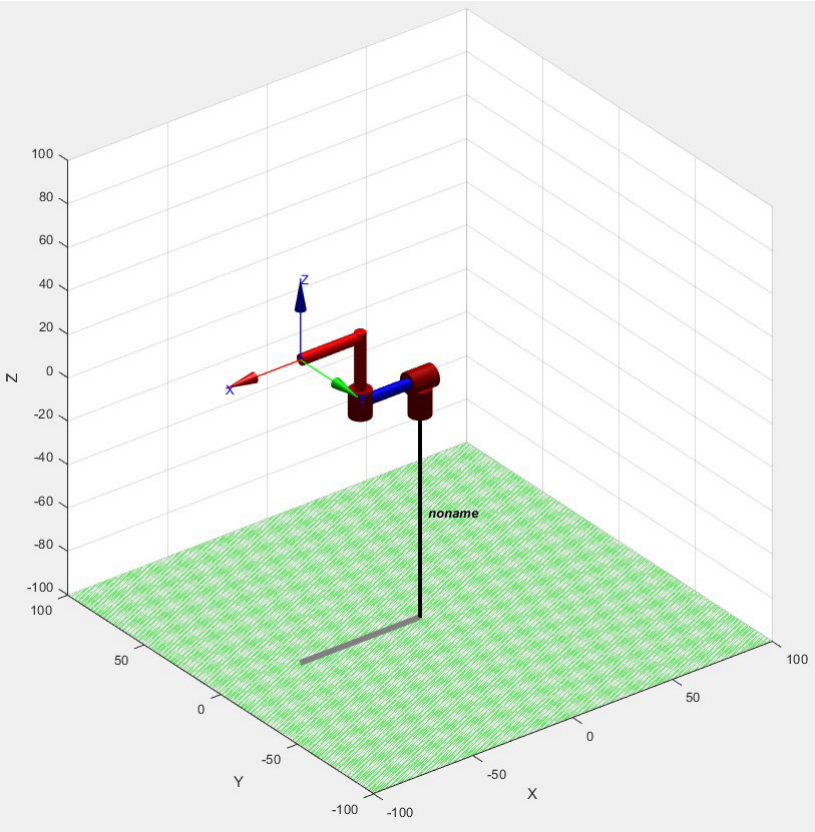


**Figure 21.** Robot Arm Plot in MATLAB

### 3.4. Inverse Kinematics

Once the DH parameters have been obtained, a code was used to get the inverse kinematics of the robot. Inverse kinematics Calculate all feasible joint angle combinations

that could be employed to achieve the end-effector of the manipulator's given position and orientation. This is a significant issue with the practical application of manipulators. [18]

### 3.5. Forward Kinematics

To get the forward kinematics of the robot, first it is necessary to get the Denavit-Hartenberg parameters from the base to the end effector, then with this matrix it is possible to find the equations in order to get the position in $x$, $y$ and set axis by giving just the angles. After putting the angles of movement of each motor, the position of the end effector with respect of the base will be obtained. In order to obtain the manipulator's singularities Jacobian matrix was calculated. From the DH parameters the homogeneous transformation matrix was obtained and eventually the Jacobian matrix for the manipulator, which helps relate the joints velocities with cartesian velocities (velocity of the tip of the robot) [18].

Once both of these parameters were calculated it was possible to use them to implement the code that allows to control the movement of the motors.

### 3.6. Artificial Intelligence

Regarding the AI part of the project an algorithm was developed in Python using OpenCV. What the algorithm does is to allow the camera to detect and count spots that may be present on a given surface. A selection of image processing tools were applied, such as gray scaling, blurring, and finding out the edges in order to achieve our goal. Making the image monochromatic is one of the most crucial processes in object detection. Thus is necessary to convert our image to a black and white tone. All object detection techniques often employ something like this. As a result, there are fewer scans, which makes the image run more quickly.

It uses the cv2.threshold function. The source picture, which should be a grayscale image, is the first parameter, the threshold value, which is used to categorize the pixel values, is the second once and the third input, maxVal, indicates the value that will

be provided if the pixel value is greater than (or occasionally lower than) the threshold value. The “THRESH_BINARY_INV” method was used because it makes the spots white and the rest black, so its easier to identify individual marks. The threshold parameters were tuned manually by trial and error. Once this is done findContours is used to detect objects and finally count the number of spots found in the image [19] [20] [21]. This can be better understood in the diagram of Fig. 22

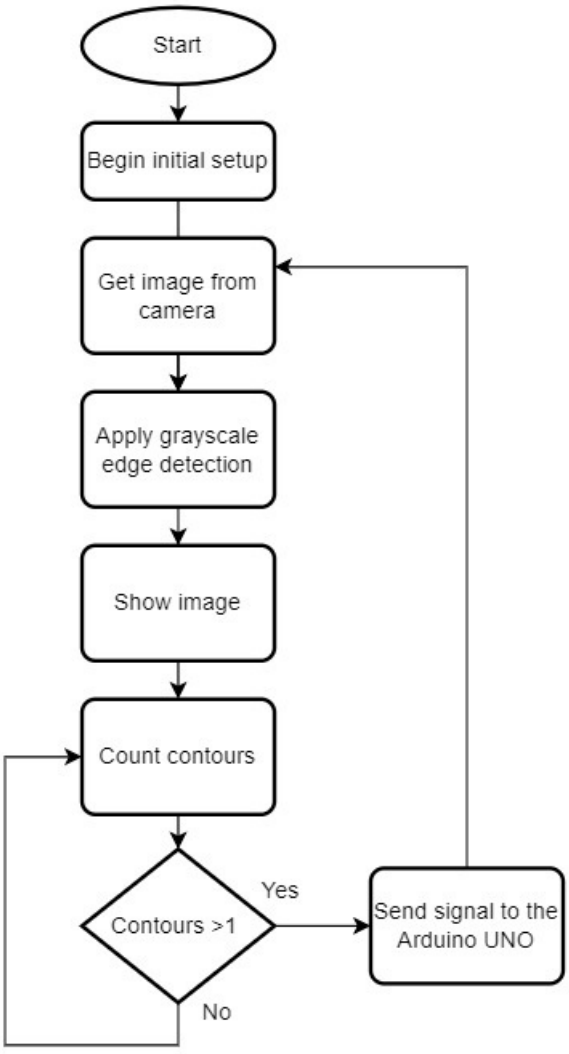


**Figure 22.** Artificial Vision Algorithm Architecture

## 4. Expenses

The total cost of making this project was approximately $ 265, which is described in Table 16 below.

**Table 16.** Total Expenses

| Component | Quantity | Unitary Cost[$] | Total [$] |
|---|---|---|---|
| 12V - 10A Power Supply | 1 | 10 | 10 |
| Raspberry Pi 4 | 1 | 50 | 50 |
| Arduino UNO | 1 | 15 | 15 |
| Cooling kit for Raspberry Pi | 1 | 7 | 7 |
| USB Web Cam | 1 | 9 | 9 |
| PVC Pipes (3m) | 1 | 3 | 3 |
| R385Diaphragm Pump | 1 | 10 | 10 |
| Step down XL4005 5A | 2 | 4 | 8 |
| FT5325M Servo Motor | 3 | 25 | 75 |
| UV Light | 1 | 15 | 15 |
| Silicone 6mm hoze (4m) | 1 | 2.5 | 2.5 |
| Bronze nozzle | 1 | 3.5 | 3.5 |
| PLA (1kg) | 2 | 20 | 40 |
| PCB (Copper Bakelite and acid) | 1 | 7 | 7 |
| PCB Components and cable | 1 | 5 | 5 |
| Nuts and Bolts | 1 | 5 | 5 |
| Total | | | $265 |

# REFERENCES


[1] "What kinds of industrial robots are there? a guide on the features of the major 6 types," *Kawasaki.*, 2018.

[2] C. Bernier, "Robotic arms: Different types and when to use them," *HowToRobot.*, 2022.

[3] M. Long, "What is a robotic manipulator? a guide," *EVS Robots.*, 2021.

[4] eTechnophiles. Guide to nema 17 stepper motor dimensions, wiring pinout. [En línea]. Disponible: https://www.etechnophiles.com/guide-to-nema-17-stepper-motor-dimensions-wiring-pinout/ (2022)

[5] P. Technologies. What is a motion control system. [En línea]. Disponible: https://prodrive-technologies.com/motion/articles/what-is-a-motion-control-system/ (2020)

[6] *12V, 0.35A AD20P-1230A Brushless Water Pump*, 2019.

[7] *6-12V, 0.7A R385 Diaphragm Pump*, 2016.

[8] *9V, 0.2A LBD WP02 Water Pump*, 2020.

[9] Z. Oksiuta, M. Jalbrzykowski, J. Mystkowska, E. Romanczuk, y T. Osiecki, "Mechanical and thermal properties of polylactide (pla) composites modified with mg, fe, and polyethylene (pe) additives," *Polymers*, vol. 12, no. 12, p. 2939, 2020.

[10] P. Dutta y U. Vaidya, "A study of the long-term applications of vinyl sheet piles," 01 2003.

[11] J. P. Vidosic, *Machine design projects*, 1957.

[12] R. G. Budynas, J. K. Nisbett *et al.*, *Shigley's mechanical engineering design*. McGraw-Hill New York, 2011, vol. 9.

[13] R. P. T. L. 2019, "Raspberry pi 4 model b datasheet," 01 2019.

[14] Arduino, "Arduino uno r3 datasheet," 01 2017.

[15] “Tip120, tip121, tip122 (npn); tip125, tip126,tip127 (pnp) plastic medium-power complementary silicon transistors,” 11 2014.

[16] A. B. Rehiara, “Kinematics of adeptthree robot arm,” in *Robot Arms*, S. Goto, Ed. Rijeka: IntechOpen, 2011, ch. 2. [En línea]. Disponible: https://doi.org/10.5772/17732

[17] A. Dictionaries y Encyclopedias. Robot kinematics. [En línea]. Disponible: https://en-academic.com/dic.nsf/enwiki/655664 (2010)

[18] J. J. Craig, *Introduction to robotics*. Pearson Educacion, 2006.

[19] A. Mordvintsev y K. Abid, “Opencv-python tutorials documentation,” *Obtenido de https://media. readthedocs. org/pdf/opencv-python-tutroals/latest/opencv-python-tutroals. pdf*, 2014.

[20] A. Sharma, J. Pathak, M. Prakash, y J. Singh, “Object detection using opencv and python,” in *2021 3rd International Conference on Advances in Computing, Communication Control and Networking (ICAC3N)*. IEEE, 2021, pp. 501–505.

[21] F. Jalled y I. Voronkov, “Object detection using image processing,” *arXiv preprint arXiv:1611.07791*, 2016.